



UNIVERSITY OF LEEDS

This is a repository copy of *A parametric study of the drying process of polypropylene particles in a pilot-scale fluidized bed dryer using Computational Fluid Dynamics*.

White Rose Research Online URL for this paper:  
<http://eprints.whiterose.ac.uk/157495/>

Version: Accepted Version

---

**Article:**

Nabizadeh, A, Hassanzadeh, H, Asadieraghi, M et al. (4 more authors) (2020) A parametric study of the drying process of polypropylene particles in a pilot-scale fluidized bed dryer using Computational Fluid Dynamics. *Chemical Engineering Research and Design*, 156. pp. 13-22. ISSN 0263-8762

<https://doi.org/10.1016/j.cherd.2020.01.005>

---

© 2020 Institution of Chemical Engineers. Published by Elsevier B.V. All rights reserved. This manuscript version is made available under the CC-BY-NC-ND 4.0 license <http://creativecommons.org/licenses/by-nc-nd/4.0/>.

**Reuse**

This article is distributed under the terms of the Creative Commons Attribution-NonCommercial-NoDerivs (CC BY-NC-ND) licence. This licence only allows you to download this work and share it with others as long as you credit the authors, but you can't change the article in any way or use it commercially. More information and the full terms of the licence here: <https://creativecommons.org/licenses/>

**Takedown**

If you consider content in White Rose Research Online to be in breach of UK law, please notify us by emailing [eprints@whiterose.ac.uk](mailto:eprints@whiterose.ac.uk) including the URL of the record and the reason for the withdrawal request.



[eprints@whiterose.ac.uk](mailto:eprints@whiterose.ac.uk)  
<https://eprints.whiterose.ac.uk/>

1 **A Parametric Study of the Drying Process of Polypropylene Particles**  
2 **in a Pilot-Scale Fluidized Bed Dryer using Computational Fluid**  
3 **Dynamics**

4 **Ali Nabizadeh<sup>a</sup>, Hossein Hassanzadeh<sup>b</sup>, Masoud Asadieraghi<sup>c</sup>, Ali Hassanpour<sup>d</sup>, Daryoush Moradi<sup>c</sup>,**  
5 **Mostafa Keshavarz Moraveji<sup>e\*</sup>, Mahdi Hozhabri Namin<sup>f</sup>**

6 a Institute of GeoEnergy Engineering, School of Energy, Geoscience, Infrastructure and Society, Heriot-Watt  
7 University, Edinburgh, UK

8 b Department of Chemical Engineering, Laval University, Quebec, QC, Canada, G1V 0A6, Canada.

9 c National Petrochemical Company (NPC), Petrochemical Research and Technology Company (NPC-RT),  
10 Arak Center, Arak, Iran

11 d School of Chemical and Process Engineering, University of Leeds, Leeds LS2 9JT, UK

12 e Department of Chemical Engineering, Amirkabir University of Technology (Polytechnic of Tehran),  
13 Tehran, 15875-4413, Iran

14 f Department of ThermoFluid, Mechanical engineering, Universiti Teknologi Malaysia, Johor Bahru,  
15 Malaysia

16

17 \*Corresponding author email: Moraveji@aut.ac.ir

18

19 **Abstract**

20 Fluidized Bed Dryer (FBD) is one of the efficient methods for drying moist particulate  
21 products. At the same time, the design and optimization of a full industrial scale FDB requires  
22 extensive studies. Using a pilot-scale dryer can be deemed as an efficient tool to obtain essential  
23 information on the drying phenomenon. Although these kinds of experimental analyses can  
24 provide valuable insight, there are still some operational limitations, including high-pressure or  
25 high-temperature conditions, which make the use of a computational procedure highly desirable.  
26 In this study, Computational Fluid Dynamics (CFD) approach has been employed to investigate a  
27 dryer. The results of numerical simulations were verified using the experimental data obtained  
28 from a pilot-scale dryer. The present investigation aims to study the effects of different operating

1 conditions. It was observed that the impacts of gas inlet temperature were negligible, as the dryer  
2 was equipped with a thermal jacket, while the gas injection velocity had significant effects on the  
3 dryer's performance. Moreover, the efficiencies of the conical and horizontal gas distributors were  
4 compared and it was concluded that the conical configuration results in better performance. The  
5 numerical and experimental investigation from this study can facilitate the design and scale-up of  
6 an industrial dryer plant.

7

8 Keywords: Fluidized bed dryer, Computational Fluid Dynamics, Drying technology, Moisture

9

## 10 **1. Introduction**

11

12 A considerable range of industrial products in different sectors experience the drying  
13 process at some stages of their production. A wide range of industrial dryers for materials with  
14 different characteristics are introduced in the literature, including fluidized bed dryers ([Hovmand,  
15 1995](#)), indirect dryers ([Devahastin and Mujumdar, 2007](#)), drum dryers ([Tang et al., 2003](#)), spray dryers  
16 ([Baker and McKenzie, 2005](#)), rotatory dryers ([Baker, 1988](#)), spouted bed dryers ([Szafran et al., 2005](#)),  
17 solar dryers ([Pangavhane et al., 2002](#)), freeze dryers ([Tang et al., 2005](#)), microwave ([Manickavasagan  
18 et al., 2006](#)), dielectric dryers ([Schiffmann, 1995](#)), infrared dryers ([Sadin et al., 2014](#)), pneumatic  
19 dryers ([Korn, 2001](#)), conveyor dryers ([Hepbasli et al., 2010](#)), superheated dryers ([Mujumdar, 1995](#)),  
20 and impingement dryers ([Aust et al., 1997](#)). To design an industrial dryer, an adequate  
21 understanding of the system such as chemical and physical reactions as well as properties and  
22 characteristics of materials are mandatory. Usually, these critical parameters are obtained from  
23 extensive experiments, usually from pilot plant scales and analyzed to optimize the design and  
24 process conditions for real industrial cases. Nevertheless, the aforementioned approach requires  
25 extensive trial and errors, manpower with high running costs and could impose health, safety and  
26 environmental risk.

27

1 Fluidized Bed Dryers (FBD) are in particular applied in different industries such as  
2 chemicals production, foodstuff, biomaterials, polymer production, and carbohydrates to dry  
3 powders and granular products. One of the most important advantages of these dryers is that in the  
4 process of drying, proper mixing occurs which improves the efficiency of drying. Another  
5 advantage is their thermal efficiency in comparison with other drying techniques, making them  
6 somewhat easier to control. Despite all the advantages, these dryers have high electrical power  
7 consumption and have limitations on particles size (100-2000  $\mu\text{m}$ ) ([Mujumdar, 2006](#))

8 Polypropylene is one of the thermoplastic polymers that can be used in different industries,  
9 such as plastic manufacturing, textiles, and medical devices. To demonstrate its importance, it  
10 should be noted that this material is the world's second-most widely produced synthetic plastic  
11 ([Pubns, 1996](#)). Polypropylene production is costly, and also a challenging process, which can be  
12 carried out with different procedures. Catalysts deactivation, finding appropriate mixing time, test  
13 designing to achieve the best mixing phenomenon, and finding the best operational conditions are  
14 among those challenges. Regardless of the method of production, one of the steps of most  
15 polypropylene processes is to deactivate catalyst residuals and strip out the dissolved monomer in  
16 the polymer using the steamer and dryer units, before they are transferred to the polymer powders  
17 silos. Nevertheless, it is widely accepted that the performance of the dryer unit has significant  
18 effects on the quality of the final products ([Pasquini and Addeo, 2005](#); [Pubns, 1996](#)).

19 The effects of different operating conditions on fluid flow within a pilot-plant dryer should  
20 be extensively investigated before the manufacturing stage. Although a pilot-plant dryer can  
21 provide valuable information, some parameters cannot be obtained due to operational limitations.  
22 For example, different gas distributors cannot be readily examined using a pilot-plant dryer  
23 because it could be a costly process. To analyze different operating conditions, including high-  
24 temperature conditions and different velocity injection cases, it is necessary to stop the system and  
25 test all designed scenarios, which is not possible at an industrial unit. To overcome this challenge,  
26 modelling approaches can be implemented to simulate the drying process in a plant with a much  
27 lower cost in comparison with experiments.

28 Numerous studies have been devoted to investigating fluid flow within dryers primarily  
29 using Computational Fluid Dynamics (CFD) methods. An extensive review study was conducted  
30 by ([Jamaledine and Ray, 2010](#)) to demonstrate the importance and popularity of CFD methods in

1 drying industries. The Eulerian-Eulerian approach was implemented by ([Antony and Shyamkumar,](#)  
2 [2016](#)) to simulate the drying of sand particles using fluidized bed dryers. The impacts of inlet air  
3 temperature on the efficiency of the dryer were investigated, and it was observed that increasing  
4 inlet temperature reduces the drying time. Mass and heat transfer in a spouted bed dryer was  
5 predicted by ([Szafran and Kmiec, 2004](#)) using CFD method. They observed a good agreement  
6 between their Eulerian-Eulerian simulation results and the experimental data. This agreement  
7 demonstrated the capability of the Eulerian-Eulerian approach for addressing this kind of problem.  
8 ([Szafran et al., 2005](#)) investigated fluid flow in a spouted-bed dryer with a draft tube. Their  
9 numerical solution captured the flow behavior of experimental data. ([Wang et al., 2008](#)) studied a  
10 complex air-solid flow within a batch fluidized bed dryer using mathematical modeling, CFD  
11 methods, and Electrical Capacitance Tomography (ECT) measurement. The results of these  
12 techniques were compared with the available experimental data, and an acceptable agreement was  
13 observed. They also presented an online process control system using CFD and ECT methods. The  
14 Eulerian-Lagrangian method was implemented by ([Fries et al., 2011](#)) to investigate fluid dynamics  
15 in a fluidized bed. The collision behavior was taken into consideration, and the effects of granulator  
16 configurations with different residence time were studied. Three-dimensional gas-solid flow in  
17 spouted beds was studied by ([Zhonghua and Mujumdar, 2008](#)) using the Eulerian-Eulerian approach.  
18 Flow instabilities and their reasons were investigated, and it was recommended that these analyses  
19 could provide valuable insight into the process design. ([Khomwachirakul et al., 2016](#)) combined CFD  
20 methods with the discrete element method (DEM) to simulate gas-solid flow within an impinging  
21 stream dryer. The results of this CFD-DEM method were compared with the conventional CFD  
22 method and experimental data. It was observed that there is a better agreement between CFD-DEM  
23 methods and experimental data because this method considers solid-solid interactions. Generally,  
24 CFD-DEM is a more complicated and costly approach that is at the moment suitable for in-depth  
25 study of simple configurations, while based on currently available computational power CFD is  
26 could be a better choice for large and complicated geometries with the multiphase flow.  
27 ([Arastoopour et al., 2017](#)) presented comprehensive study and reported that Kinetic Theory of  
28 Granular Flow (KTGF) could be adequate for simulating fluid-solid problems using Eulerian-  
29 Eulerian approach. A circulating fluidized bed (CFB) reacting loop was studied numerically using  
30 CFD methods considering gas-solid flow by ([Ghadirian et al., 2019](#)). KTGF was used to consider  
31 solid particles motion, where excellent agreement between the numerical simulations and

1 experimental was observed. In addition to particle-fluid systems, Eulerian-Eulerian approach  
2 based on KTGF was also used for particle segregation in a rotating drum by ([Huang and Kuo, 2018](#))  
3 and granulation process within a high shear mixer granulator by ([Ng et al., 2009](#)). A good agreement  
4 between experimental results and numerical simulations was observed. Overall, it can be  
5 concluded that Eulerian-Eulerian approach could adequately address solid-gas systems, where full  
6 Eulerian- Lagrangian approach would be costly and inefficient.

7 In this study, a three-dimensional pilot-plant fluidized bed dryer was investigated both  
8 experimentally and numerically. This research is an optimization study of a specific industrial  
9 drying plant working in a petrochemical unit. To the best of our knowledge, no previous work on  
10 this particular dryer has been reported, particularly on the simulation study of three-phase flow in  
11 the drying process of polymerization. A numerical simulation based on CFD was developed to  
12 investigate the effects of different operating conditions related to the injecting gas phase. First, the  
13 accuracy of this proposed numerical solution was verified by the experimental data obtained from  
14 a pilot-plant fluidized bed dryer. In the next step, the effects of initial temperature, initial moisture,  
15 the velocity of the injecting gas, and two different types of gas distributors were analyzed. These  
16 parameters are playing crucial roles, and significantly affect the efficiency of a dryer plant. The  
17 combination of this numerical simulation with the experimental pilot plant data can be used to  
18 design and optimize an industrial dryer plant.

19

## 20 **2 Methodology**

21 In this study, a three-dimensional numerical scheme using CFD method was developed to  
22 analyze multiphase flow within a fluidized bed dryer plant, and the accuracy of these numerical  
23 simulations was verified against experimental data. After verification, sets of numerical  
24 simulations were conducted to analyze the critical parameters to propose an optimum operating  
25 condition.

### 26 **2.1 Governing Equations**

27 Two methods, including Eulerian-Eulerian and Eulerian-Lagrangian, can be utilized to  
28 simulate multiphase flow during a drying process. In both approaches, the displacing phase (e.g.,

1 gas phase) is assumed as a continuous phase. In the Eulerian-Eulerian approach, displaced phase  
 2 or solid phase is assumed as a continuous phase as well. However, in the Eulerian-Lagrangian  
 3 approach, solid phase is assumed as a dispersed phase. In this method, all particles are simulated  
 4 separately. This industrial system comprises of 1,641,000 discretized cells and more than  
 5 40,000,000 particles, which is very computationally demanding. This research is a parametric  
 6 study with various transient simulations; therefore, implementing Eulerian-Lagrangian approach  
 7 (CFD-DEM) seems unnecessary or somewhat impossible with the available computational  
 8 resources.

9 In this study, a three dimensional CFD method assuming Eulerian-Eulerian-Eulerian flow  
 10 was then implemented to determine fluids distribution in the system. In this regard, ANSYS Fluent  
 11 has been used as the modeling tool. To simulate gas-solid-liquid behavior, the KTGF theory was  
 12 implemented for solid interactions, where mass transfer and drag forces were taken into account.  
 13 The governing equations are described extensively in the following subsections.

14 ***Continuity equation:***

$$\frac{\partial}{\partial t}(\alpha\rho) + \nabla \cdot (\alpha\rho\vec{v}) = M_{gl} \quad (1)$$

$$\frac{\partial}{\partial t}(\alpha_s\rho_s) + \nabla \cdot (\alpha_s\rho_s\vec{v}_s) = 0 \quad (2)$$

15

16 Where  $M_{gl}$  describes the volumetric mass transfer from the liquid to the continuous gas phase.

17 ***Momentum equation: (for each phase)***

$$\frac{\partial}{\partial t}(\alpha\rho\vec{v}) + \nabla \cdot (\alpha\rho\vec{v}_i\vec{v}_j) = -\alpha\nabla P + \nabla \cdot \vec{\tau} + \alpha\rho\vec{g} + M \quad (3)$$

$$\vec{\tau} = \alpha\mu(\nabla\vec{v} + \nabla\vec{v}^T) + \alpha(\lambda - \frac{2}{3}\mu)\nabla \cdot \vec{v}\vec{I} \quad (4)$$

18 To demonstrate the volumetric interactions between phases,  $M$  is added to the continuity  
 19 equation.

20

21 ***Kinetic theory of granular flow (KTGF):***

1 To improve our understanding of fundamental behaviors of flow containing solid particles,  
 2 proper values should be assigned to the solid phase properties. Since there is no direct measurement  
 3 method, a reliable estimation method should be used. To overcome this challenge, constitutive  
 4 equations which were derived based on the kinetic theory are presented below.

5 Solid pressure:

$$P_s = 2\rho_s(1+e_s)\alpha_s^2 g_0 \theta_s \quad (5)$$

6 Granular temperature:

$$\frac{2}{3} \left[ \frac{\partial}{\partial t} (\rho_s \alpha_s \theta_s) + \nabla \cdot (\rho_s \alpha_s \theta_s \bar{v}_s) \right] = (-\nabla P_s \bar{I} + \bar{\tau}_s) : \nabla \bar{v}_s + \nabla \cdot (k_{\theta_s} \nabla \theta_s) - \gamma_s + \phi_\theta \quad (6)$$

7 Solid shear stress:

$$\mu_s = \mu_{s,col} + \mu_{s,kin} + \mu_{s,fric} \quad (7)$$

8 Solid bulk viscosity:

$$\lambda_s = \frac{4}{3} \alpha_s \rho_s d_s g_0 (1+e_s) \left( \frac{\theta_s}{\pi} \right)^{\frac{1}{2}} \quad (8)$$

9 Where:

$$g_0 = \left[ 1 - \left( \frac{\alpha_s}{\alpha_{s,max}} \right)^{\frac{1}{3}} \right]^{-1} \quad (9)$$

$$\theta_s = \frac{1}{3} \overline{\mu'_s \mu'_s} \quad (10)$$

### 10 **Drag model:**

11 Interaction forces between phases were summarized on the right-hand side of the  
 12 momentum equation. These forces can be divided into drag forces, mass forces, and lift forces.  
 13 ([Rafique et al., 2004](#); [Sokolichin et al., 2004](#)) demonstrated that drag forces are playing a more crucial  
 14 role than other forces. Therefore, in this study, we merely considered the drag forces, and the  
 15 impacts of other forces were neglected. In this study, gas-solid and gas-liquid drag forces were  
 16 considered, but liquid-solid drag forces were neglected.

### 17 **Gas-liquid drag force:**

18 The Schiller-Naumann model ([Schiller and Naumann](#)) was implemented which is widely used in  
 19 literature for this kind of problems ([Ochieng and Onyango, 2008](#)):

$$f = \frac{C_D \text{Re}}{24} \quad (11)$$

1 And the drag coefficient is:

$$C_D = \frac{24}{\text{Re}_l} [1 + 0.15(\text{Re}_l)^{0.687}] \quad \text{Re} \leq 1000 \quad (12)$$

$$C_D = 0.44 \quad \text{Re} \geq 1000 \quad (13)$$

2 It should be noted that the Reynolds number should be calculated based on the following equation:

$$\text{Re} = \frac{\rho_l d_l |\vec{v}_l - \vec{v}_g|}{\mu_g} \quad (14)$$

3 **Solid-gas drag force:**

4 In this section, Gidaspow's equation ([Gidaspow et al., 1991](#)) is used:

$$K_{sg} = \frac{3}{4} C_D \frac{\alpha_s \alpha_g \rho_g |\vec{v}_s - \vec{v}_g|}{d_s} \alpha_g^{-2.65} \quad \alpha_l > 0.8 \quad (15a)$$

$$K_{sg} = 150 \frac{(1 - \alpha_g)^2 \mu_g}{\alpha_g d_s^2} + 1.75 \frac{(1 - \alpha_g) \rho_g |\vec{v}_s - \vec{v}_g|}{d_s} \quad \alpha_l < 0.8 \quad (15b)$$

5 Where

$$C_D = \frac{24}{\alpha_l \text{Re}_s} [1 + 0.15(\alpha_l \text{Re}_s)^{0.687}] \quad \text{Re}_s < 1000 \quad (16a)$$

$$0.44 \quad \text{Re}_s > 1000 \quad (16b)$$

6

7 The Reynolds number can be calculated using the following equation:

$$\text{Re}_s = \frac{\rho_p d_s |\vec{v}_s - \vec{v}_g|}{\mu_g} \quad (17)$$

8 **Energy equation:**

9 Energy equations are considered because there is heat transfer between these phases. The  
10 energy equation for gas-solid is written as:

$$\frac{\partial}{\partial t}(\alpha \rho c_p T) + \nabla \cdot (\alpha \rho c_p v T) = \nabla \cdot (\alpha k \nabla T) + M_h \quad (18)$$

1

2 In **Eq. 18**,  $M_h$  represents the volumetric heat source in the system. For the gas-solid system we  
3 have:

$$M_h = \sum \frac{6(\alpha - 1)}{d_p} h (T_p - T_g) \quad (19)$$

4 Gas-solid heat transfer coefficient can be calculated using the following equation ([Gunn, 1978](#)):

$$Nu = (7 - 10\alpha_f + 5\alpha_f^2) (1 + 0.7 Re_s^{0.2} Pr^{1/3}) + (1.33 - 2.4\alpha_f + 1.2\alpha_f^2) Re_s^{0.7} Pr^{1/3} \quad (20)$$

5 where

$$Pr = \frac{c_p \mu}{k_g} \quad (21)$$

6 Finally, particle temperature is obtained by the following equation:

$$m_p c_p \frac{\partial T_p}{\partial t} = h_v \frac{\partial m_p}{\partial t} + h A_p (T_g - T_p) \quad (22)$$

7

## 8 **2.2 Plant Geometry, Boundary Conditions, and Solution Methods**

9 The pilot plant dryer used in this study has a cylindrical shape with 1.15 m<sup>3</sup> volume and 12  
10 mm stainless steel wall, as presented in **Fig. 1**. The equipment has two inlets for wet particles and  
11 high-temperature gas, and two outlets for dry particles and wet gas. It is also equipped with  
12 thermometers and gamma transmitters for measuring the bed height. For the simulations the  
13 configurations of geometry and boundary conditions are depicted schematically in **Fig. 2**. To  
14 ensure that our numerical simulation results are not mesh-dependent, a mesh independency  
15 analysis was conducted assuming four different mesh configurations. All simulation conditions  
16 are listed in **Table. 1**. Grid numbers for these meshes were 720k, 1322k, 1641k, and 1960k. For  
17 these configurations, moisture content at the end of simulation time was recorded. There was no

- 1 difference between the results of mesh.3 (1641K) and mesh.4 (1960K). Therefore, the mesh with
- 2 1,641,000 cells was selected for further simulations.



**Fig. 1.** Pilot plant dryer picture (top section)

3

4

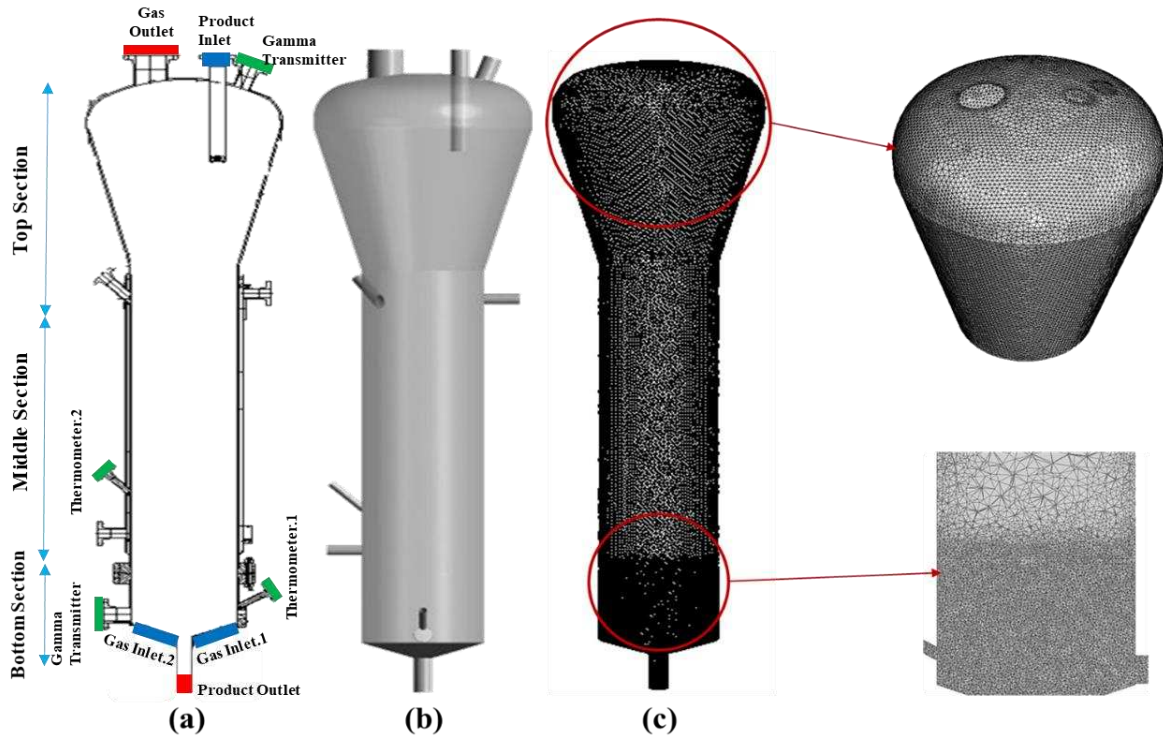


**Fig. 2.** Pilot plant dryer configuration (a) the drawing of the pilot plant dryer (b) 3D configuration (c) Mesh schematic

1

2

Different procedures and algorithms that were implemented to solve the required equations are described. The pressure-velocity equations were coupled using SIMPLE (Semi-Implicit Method for Pressure-Linked Equations) algorithm. Momentum, Volume fraction, Energy, and pressure equations were discretized using second-order upwind, QUICK (Quadratic Upstream Interpolation for Convective Kinematics), and least-squares cell based, respectively.

7

### 8 **3 Experimental Setup**

9

In the experimental study, the drying process was observed, and the required outputs were recorded. In the following, the dryer plant and the process conditions are described.

11

#### **3.1 Physical Reactions and Procedures within the Dryer**

1 Wet particles and high-temperature gas are injected into the system from the inlet at the  
2 top and the bottom of the equipment, respectively. A mixing phenomenon between high-  
3 temperature gas and wet particles takes place, which reduces particles' moisture. In the end, the  
4 dry particles leave the plant through an outlet at the bottom of the equipment (**Fig. 2a**). The  
5 operating conditions and material properties are presented in **Table. 1**.

6 **Table. 1.** Experiment operating conditions

Parameter	Value
Operating Pressure	0.2 barg
Operating Temperature	100 ° C
Gas Injection Rate	0.4 m/s
Plant volume	1.15 m <sup>3</sup>
Solid density	905 kg/m <sup>3</sup>
Gas density	1.138 kg/m <sup>3</sup>
Bulk density	400 kg/m <sup>3</sup>
Liquid viscosity	0.001kg/m-s

7

## 8 **4 Results and Discussion**

### 9 **4.1 Experimental Data**

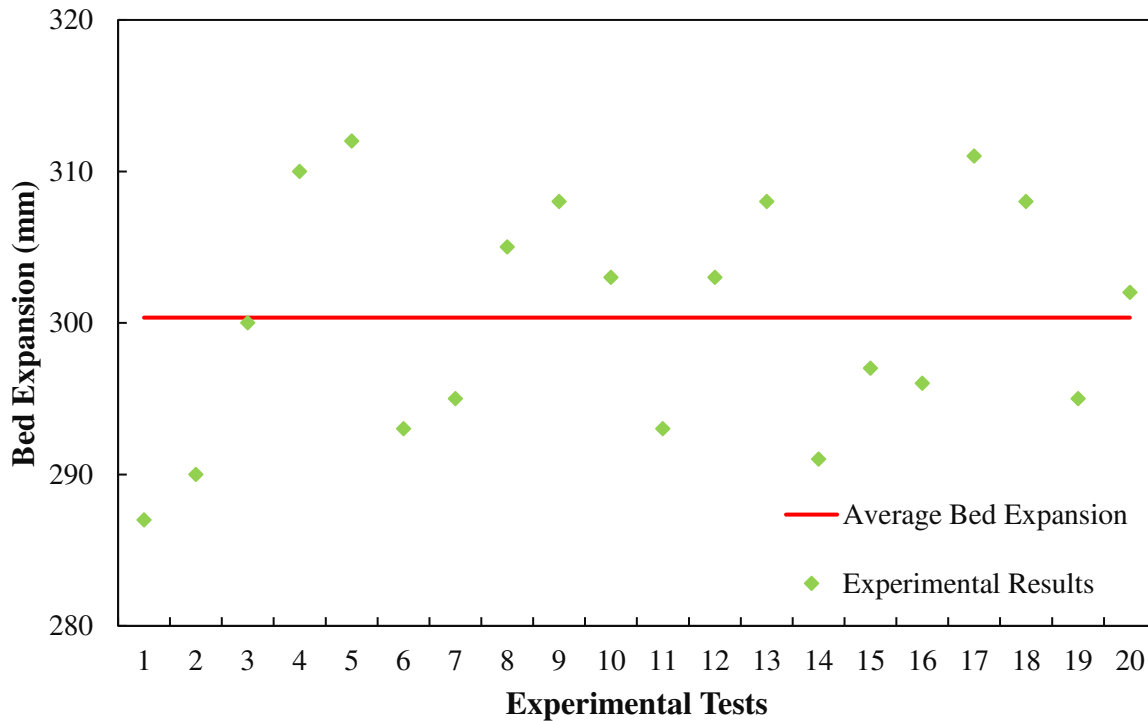
10 The experiment was conducted under the abovementioned operating conditions (**Table 1**),  
11 and two specific outputs were measured. The first one is the bed expansion inside the dryer. This  
12 parameter was determined using a gamma transmitter, which can locate particles inside the system.  
13 This dryer was also equipped with two thermometers at different locations (**Fig. 2a**), which were  
14 used to determine the temperature inside the system. These data were used to verify simulations'  
15 results in the following section.

16

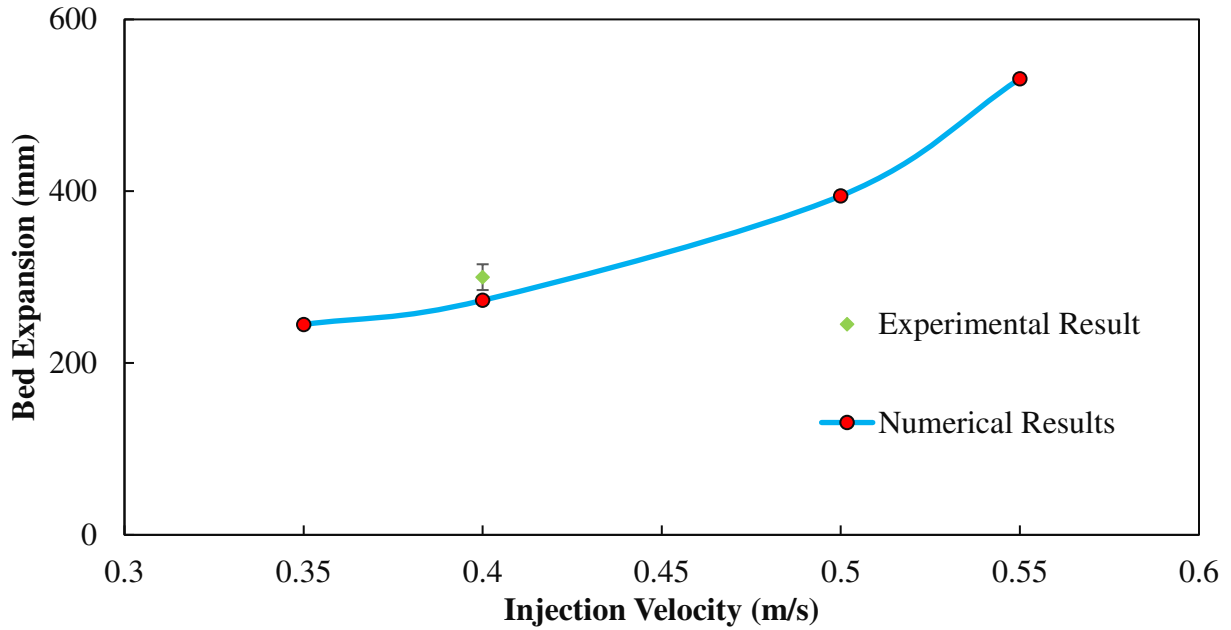
17

### 18 **4.2 Model Verification**

1 To verify this numerical scheme, the experimental finding from the pilot plant dryer was  
2 compared with the numerical simulation results. Due to operational complexity, we could not  
3 conduct experiments under different operational conditions. Altering operational conditions may  
4 be a risky and costly process for the industrial unit. The experimental result of bed expansion was  
5 therefore obtained using a gamma level transmitter under constant operating conditions, but  
6 measurements were repeated many times. **Fig 3a** depicts the bed expansion of different runs  
7 together with the averaged value for bed expansion. The standard deviation for these experiments  
8 was found to be 7.69 mm. **Fig. 3b** illustrates the bed expansion data versus gas injection velocity  
9 for four numerical simulations with different gas injection velocities together with the average bed  
10 expansion measured experimentally for one operating conditions. As illustrated in **Fig. 3b**, the  
11 numerical simulation slightly under predicts the experimental results, but the agreement between  
12 results is acceptable. Ideal conditions associated with the numerical simulation and different bed  
13 height measurement techniques can be responsible for this minor difference.



(a)



(b)

**Fig. 3.** (a) Bed expansion of different runs under similar operating conditions

(b) Bed expansion versus gas inlet velocity for numerical and the experimental data point

1

2 In the following, further simulations are carried out to determine the most effective  
 3 parameters for this particular dryer.

#### 4 **4.3 Effects of Gas Inlet Temperature**

5 The gas inlet temperature is an important parameter for evaporation of moisture in drying  
 6 technology. This fluidized bed dryer is also equipped with a thermal jacket welded to the dryer  
 7 shell to attain a uniform temperature distribution. **Fig. 4** demonstrates how the time-averaged  
 8 temperature distribution could change if the dryer was without the thermal jacket.

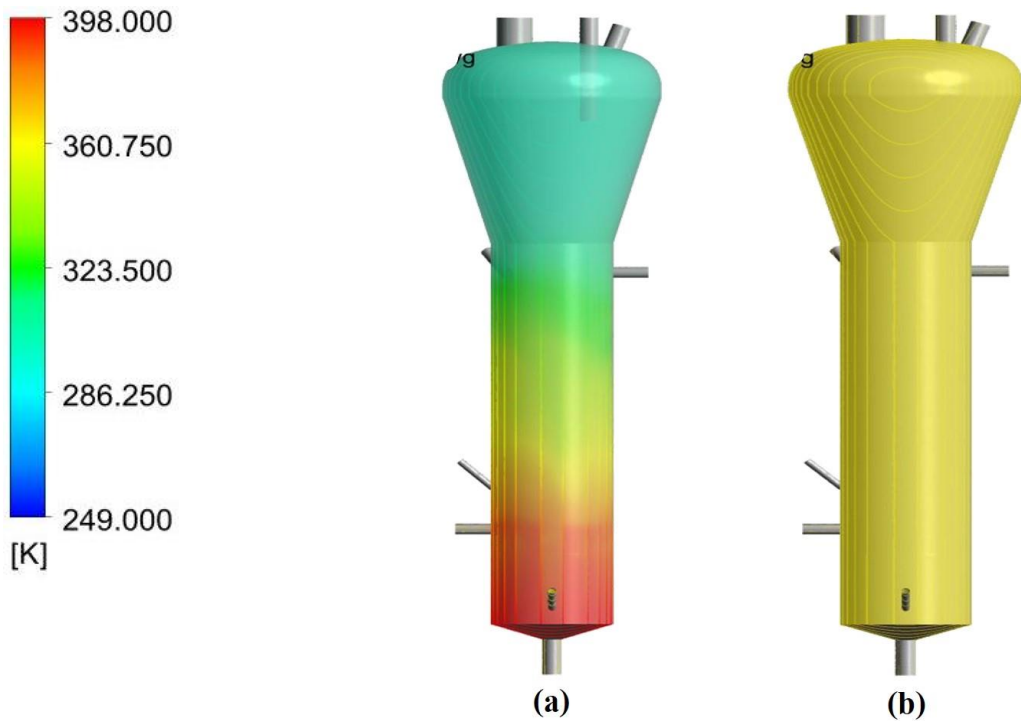


**Fig. 4.** Time-averaged temperature distribution (a) without thermal jacket (b) with thermal jacket

1

2 Non-uniform temperature distribution (**Fig. 4a**) leads to a non-uniform evaporation rate,  
 3 which significantly reduces drying efficiency, and this is inappropriate for polypropylene  
 4 production. **Fig. 4b** represented the temperature distribution of the dryer with a thermal jacket. In  
 5 this case, the nearly uniform temperature distribution is observable within the dryer.

6 As mentioned earlier, a thermal jacket was used in this pilot plant dryer. Therefore, uniform  
 7 temperature distribution was expected. During the experiment, the temperature was recorded at  
 8 two points within the pilot-plant dryer. In **Table. 2**, the results of numerical simulations are  
 9 compared with the experimental data, where a good agreement between them can be observed.

10

11 **Table. 2.** Temperature measurement; a comparison between numerical simulations and the  
 12 experimental analysis

	Temperature obtained from the experiment (°C)	Temperature obtained from the numerical simulation (°C)
Bottom of the plant (point #1)	94.5	94.4
Top of the plant (point #2)	95.0	94.8

1

2

3 Further simulations were carried out to investigate the effects of different inlet  
4 temperatures on the moisture of particles. **Fig. 5** illustrated moisture variation versus relative time.  
5 It should be noted that in these simulations, moisture converts from liquid covering the particles  
6 into the gas phase. To measure only the moisture associated with particles, we have divided this  
7 plant into three sections. These sections were specified in **Fig. 2**. The moisture content, which is  
8 used in the following figure refers to the bottom section of the dryer, near the outlet, that is filled  
9 with the particles. As evidenced by **Fig. 5**, the particle moisture was not significantly affected by  
10 the inlet temperature variation. Therefore, if necessary, it could be possible to use a lower inlet  
11 temperature (while it is not below operational limitations). However, the risk of outlet gas  
12 condensation must be considered.

13

14

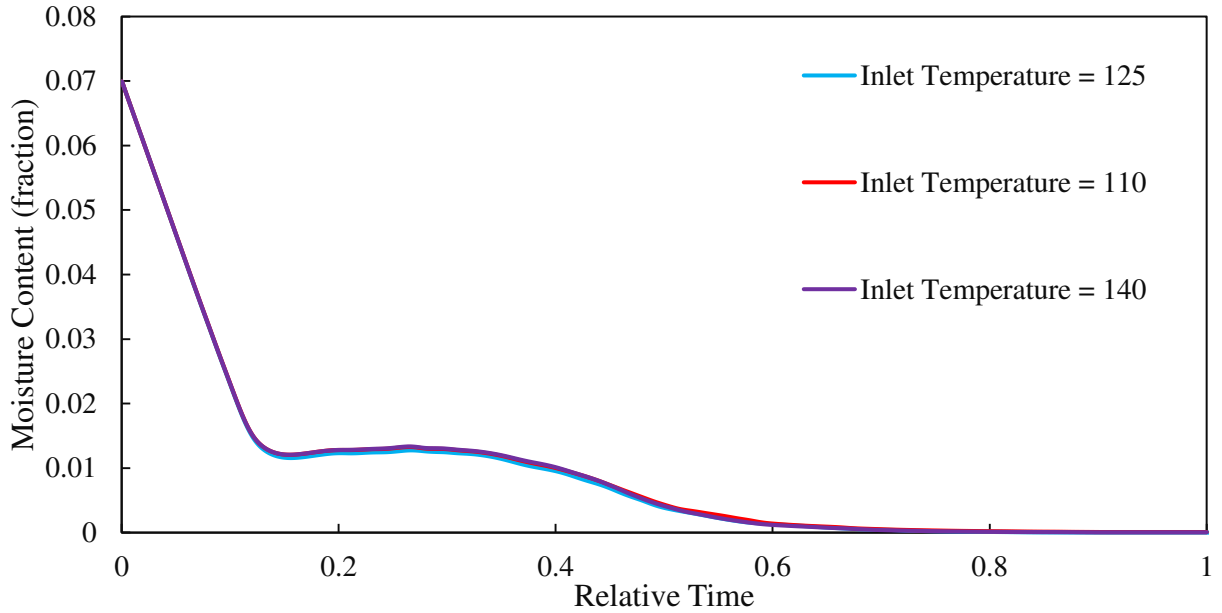


**Fig. 5.** Outlet particles moisture in different gas inlet temperature

1

## 2 **4.4 Effects of Gas Injection Velocity**

3 The gas velocity is one of the most critical parameters that could affect fluidization  
 4 regimes, the height of fluidization, and other hydrodynamic characteristics. These changes could  
 5 affect the particles moisture. **Fig. 6** illustrates the moisture content of particles in each timescale  
 6 for three different gas velocities. Similar to previous cases, the moisture content was considered  
 7 for the bottom section of the dryer. As seen, the overall behavior of the moisture content in the four  
 8 cases are similar to each other. However, at the beginning of simulations, the slop of moisture loss  
 9 (i.e., drying time) for the case with the lowest velocity is smaller than those of others. Hence,  
 10 increasing the gas velocity could be regarded as a positive effect on the dryer performance. It  
 11 should be noted that the range of velocities in this pilot plant dryer is limited (0.3-0.6 m/s). **Fig. 7**  
 12 shows a better illustration of the effects of gas velocity on the hydrodynamics.

13

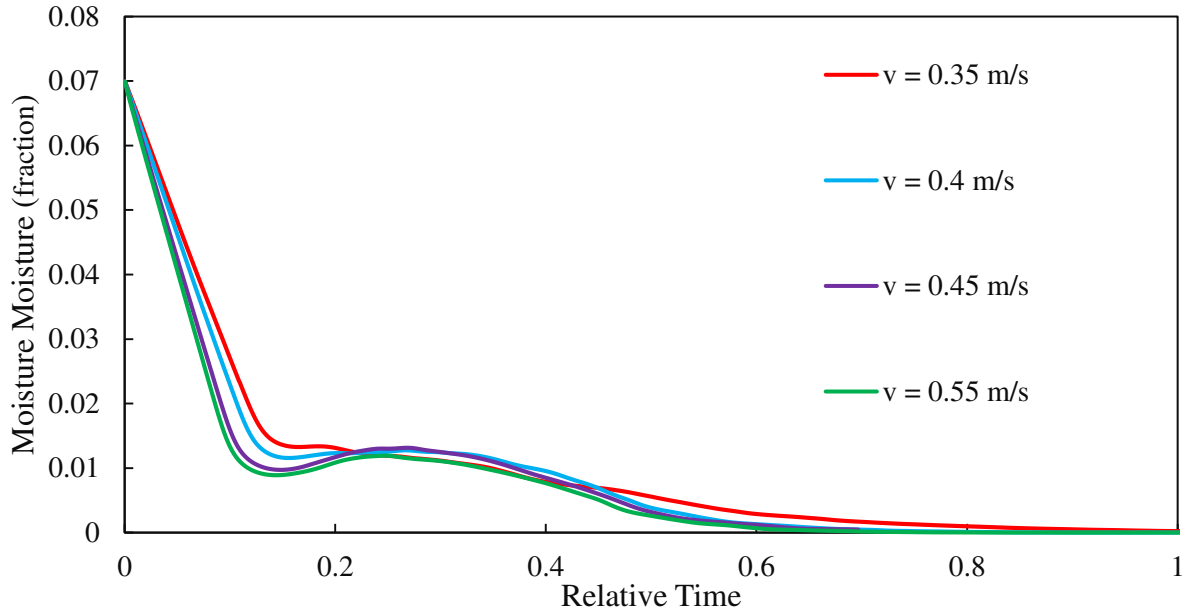


**Fig.6.** Moisture content versus time at different gas velocities

1

2

3

4

5

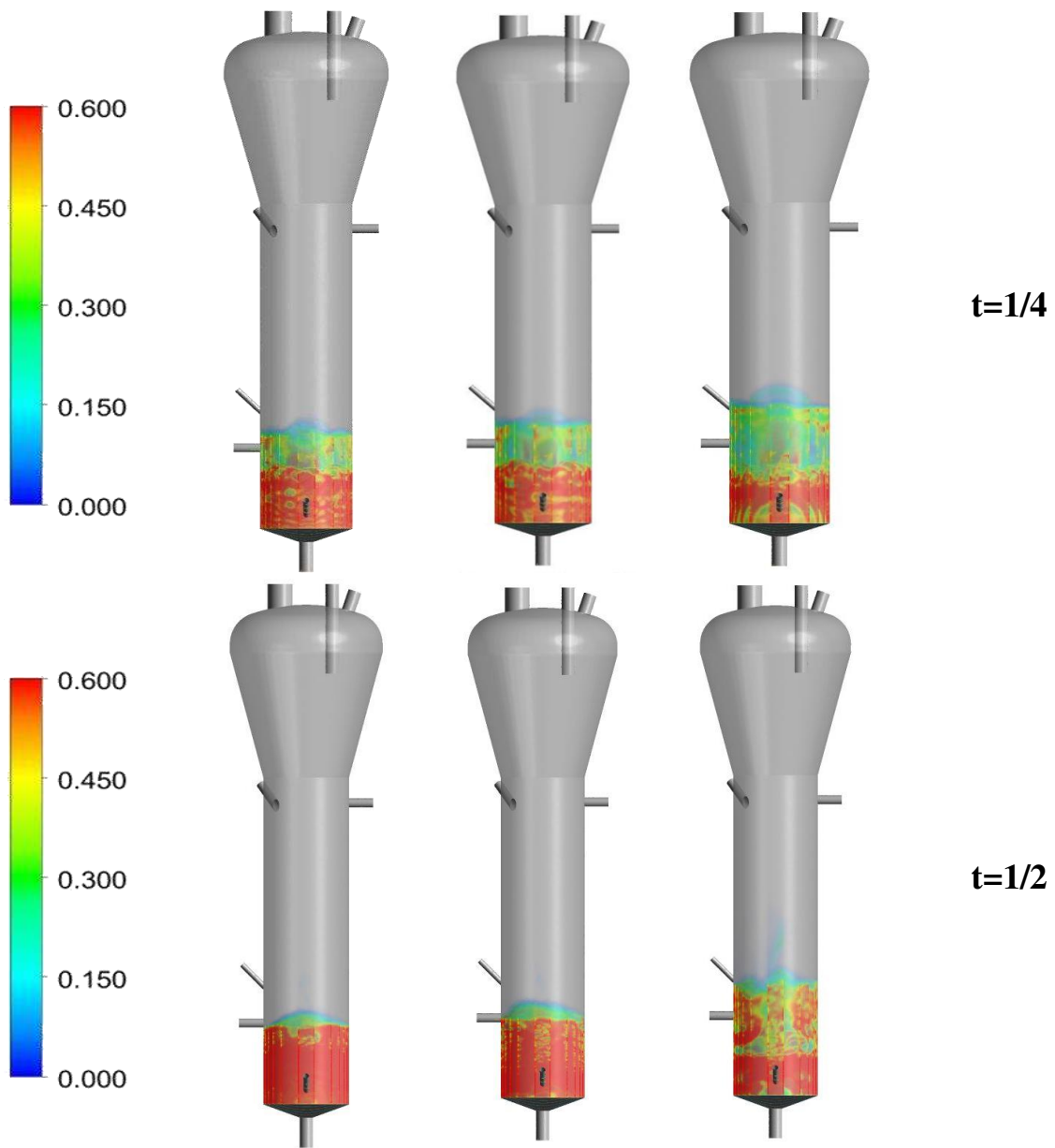
6

7

8

9

As evidenced by **Fig. 7**, the time scale of turbulence has increased for the case with  $v = 0.55$  m/s, which may not be suitable. In the first time interval ( $t = 0.25$ ), the moisture content reduction is faster for  $v = 0.55$  m/s as compared to other velocities. Based on **Fig. 6** and **Fig. 7**,  $v = 0.45$  m/s is a suitable choice for this system, because its drying time (the slope of **Fig. 6**) is not increased significantly in comparison with the case with  $v = 0.55$  m/s. Cases with higher velocities require more energy, which is not efficient while their drying time is not improved. Besides, increasing the velocity will increase the chance of particle breakage and dust production, which are not desirable.



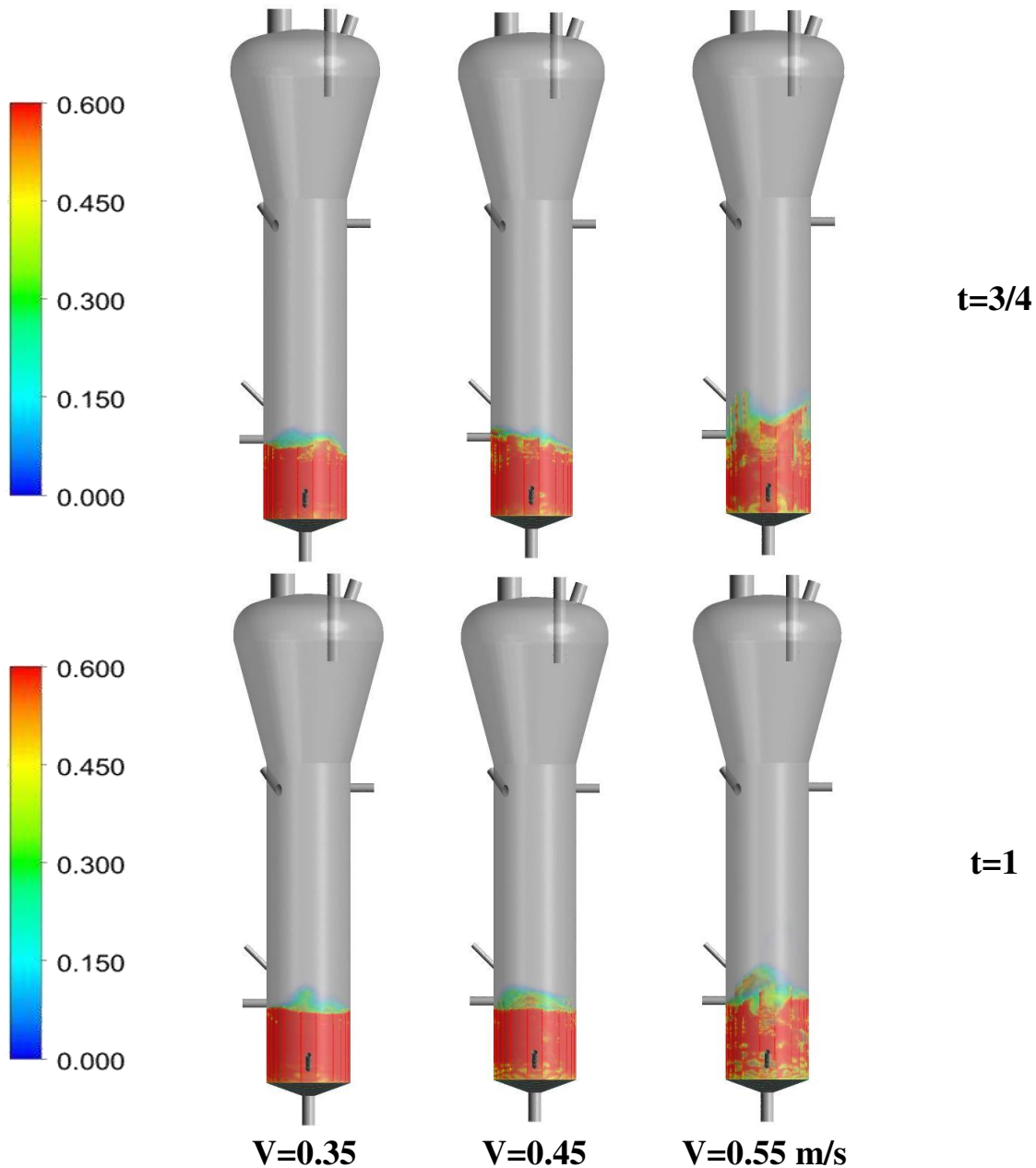


**Fig.7.** 3D contours of solid volume fraction in different gas inlet velocity

1

## 2 **4.5 Effects of gas distributors**

3 As distributors have significant effect on the hydrodynamics, they can substantially affect  
 4 the dryer efficiency. A conical shaped and a flat gas distributor, were suggested by the equipment  
 5 supplier, hence their performance was numerically investigated in this study. **Fig. 8** illustrated the  
 6 difference between the two cases at different time scales. It should be noted that other operating

1 conditions were fixed at  $v = 0.45$  m/s and inlet temperature of  $125^{\circ}\text{C}$ . The results suggest that the  
2 dryer with the flat distributor results in longer drying time as compared with the conical distributor  
3 for upper particles to take part in mixing. For example, at the time interval =  $1/4$ , in the conical  
4 distributor, upper particles participated in the mixing process, while in the flat distributor, the gas  
5 has not reached the top of bed height yet. Furthermore, under  $v = 0.45$  m/s, in the flat distributor,  
6 the height of particles is higher than that of the conical distributor, which may not be desirable. To  
7 better understand the effects of the distributor on the performance of dryers, the moisture content  
8 is studied below.

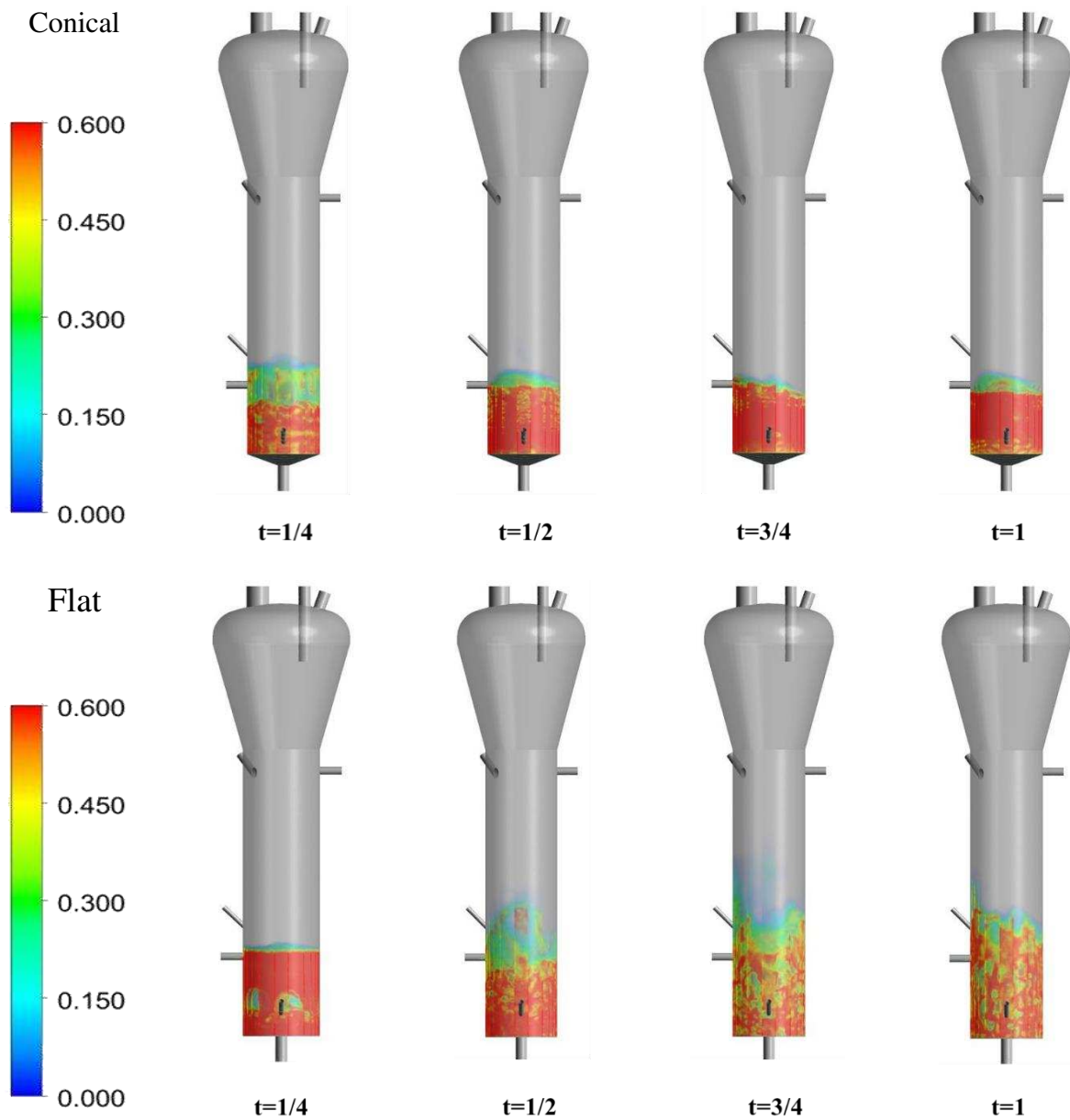


**Fig. 8.** 3D contours of solid volume fraction in the different gas distributor (Conical and Flat)

1

2 **Fig. 9** depicts particle moisture content versus time scales. As shown for the flat distributor,  
3 the moisture content is decreased at the beginning, but after  $t = 1/2$ , it is again increased. It should  
4 be noted that the results refer to the moisture content of the lower section of the dryer (near the  
5 outlet). In the beginning, the gas raises the particles, and approximately at  $t = 1/2$  the escaped gas  
6 (moist) from solids bulk together with the upper particles, including those with high moisture  
7 content, returns to the lower part of the dryer near the outlet due to the high turbulence. For this  
8 reason, the mixing time in the flat distributor is longer than the conical distributor.

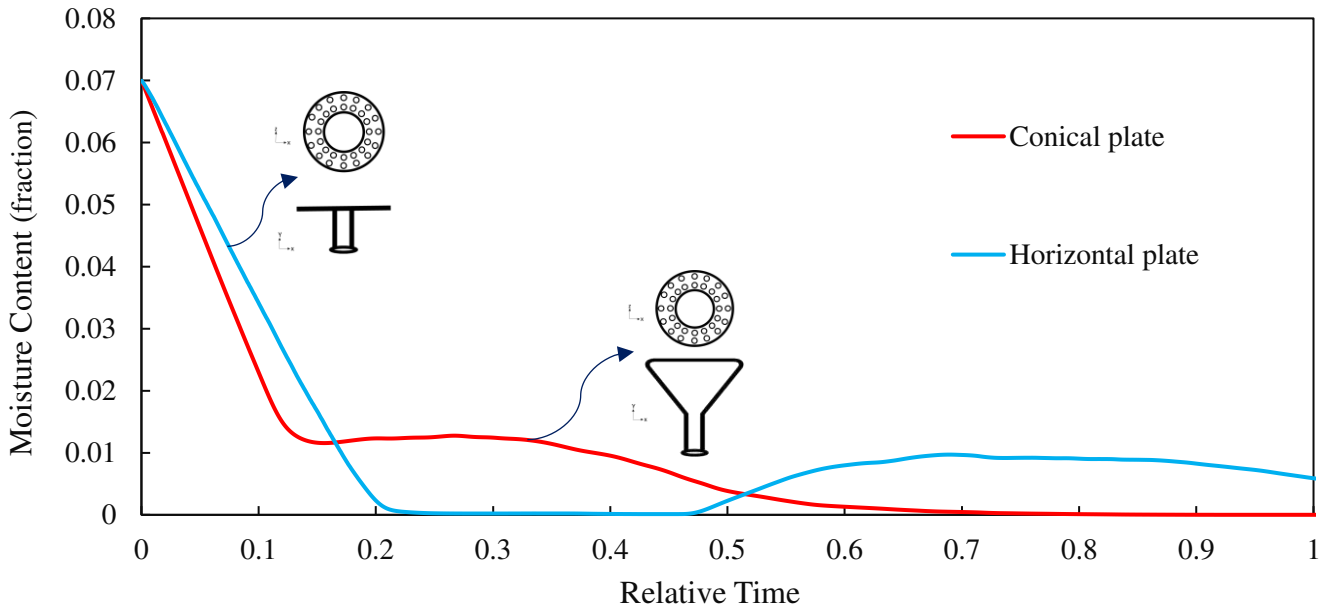


**Fig. 9.** Moisture plot versus time for two types of distributor (Conical and Flat distributor)

9

10 As mentioned above, the flat distributor is unsuitable for this type of dryer while the conical  
11 distributor could have better performance in the fluidization. The results reveal the vital role of  
12 distributor for the dryer efficiency.

13

#### 14 **4.6 Effects of Initial Particle Moisture**

1 One of the most important parameters that can significantly affect fluidized bed dryer  
2 efficiency is the initial moisture of wet particles. It is essential to know whether this plant can dry  
3 particles with high initial moisture contents, or a pre-drying process would be required. In this  
4 section, we have conducted two simulations with different initial moistures. These initial moisture  
5 values (minimum and maximum moisture of initial particles) were taken from the industrial unit.  
6 As depicted in **Fig. 10**, these two cases yield the same result, and the plant efficiency did not  
7 decrease as the initial moisture was increased. Therefore, it can be concluded that no more energy  
8 consumption is required for particles with higher initial moisture.

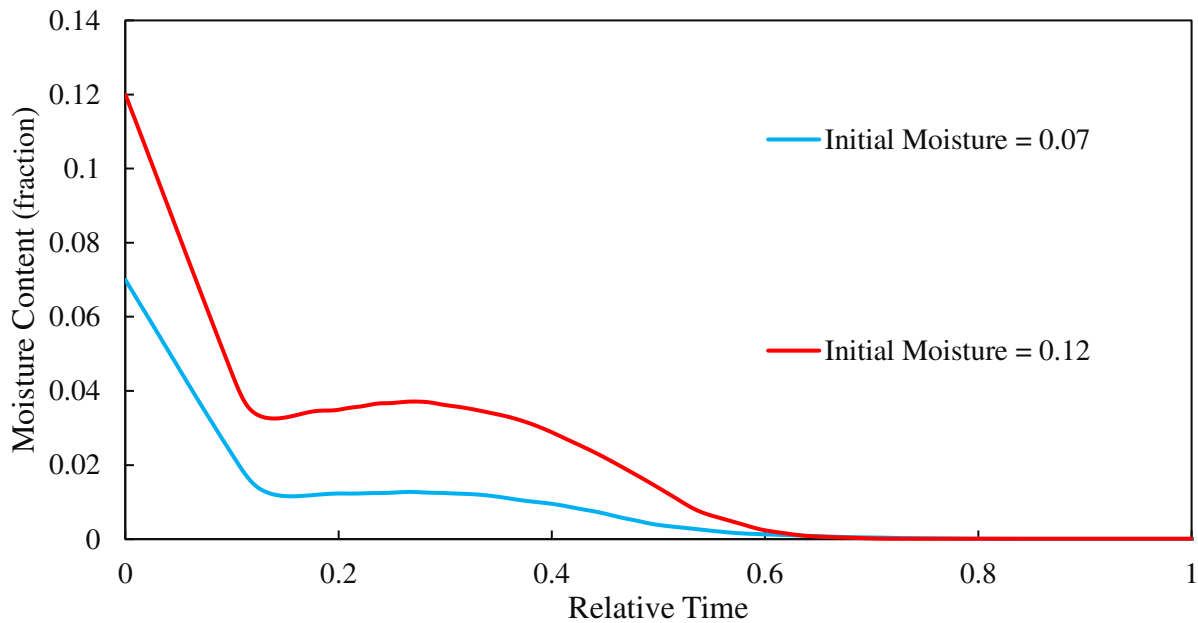


**Fig. 10.** Moisture plot versus time for two cases with different initial moisture

9

## 10 **4.7 Optimized Configuration**

11 In the numerical modeling section, we have conducted some simulations to achieve the  
12 optimum conditions for this specific fluidized bed dryer. These numerical simulations helped us  
13 to reduce the numbers of trials and errors required for designing a dryer plant. We have studied  
14 four different operating conditions, and the results are presented here. It should be noted that the  
15 best solution is the one with lower drying time and higher drying efficiency. The first parameter is  
16 the injection temperature. As evidenced by the results of this study, increasing injection  
17 temperature has no significant effects on drying efficiency due to the presence of a thermal jacket.

1 Therefore,  $T = 125\text{ }^{\circ}\text{C}$  is suitable because it reduces energy costs, and it is not below the  
2 operational limitations. Between the two different types of distributors better efficiency was  
3 observed for the conical distributor. Injection velocity was another parameter that was studied in  
4 **Section 4.4**. Different injection velocities were tested, and  $V = 0.45\text{ m/s}$  was proposed as the best  
5 solution. The inlet wet particles of this dryer unit are the outlet particles of the steamer unit. Two  
6 different moisture contents corresponding to the minimum and maximum levels of the steamer  
7 unit in practice were investigated which revealed no pre-drying process would be required for the  
8 case of maximum moisture content.

9

## 10 **5. Conclusion**

11 Experimental and numerical analyses were conducted to analyze and optimize the drying  
12 process within a pilot-plant fluidized bed dryer. To this end, the Computational Fluid Dynamics  
13 (CFD) was used to simulate fluid flow in a pilot-plant fluidized bed dryer. The model was validated  
14 by comparison with the experimental data. In particular, the bed expansion velocity was compared  
15 with the numerical results, where approximately 5% error was observed. After verification, an  
16 optimization study was carried out by conducting further simulations with different gas injection  
17 velocities, initial moisture contents, gas injection temperatures, and two different gas distributors  
18 (conical and flat types). The optimal operating conditions for the dryer used in this study are  
19 achieved for a conical distributor with the injection velocity and temperatures of 0.45 m/s and 125<sup>o</sup>  
20 C, respectively, for the feed with the initial moisture content of 0.12. The study in this work can  
21 significantly reduce the number of experimental trials and errors for achieving the optimum  
22 operating conditions of the dryer. The approach can be extended for the design and scale-up of an  
23 industrial dryer in future studies.

24

## 25 **Nomenclatures:**

$\alpha$	Volume fraction []
$\rho$	Density [ $\text{kg.m}^{-3}$ ]

V	Velocity [ $\text{m}\cdot\text{s}^{-1}$ ]
$\mu$	Viscosity [ $\text{kg}\cdot\text{m}^{-1}\cdot\text{s}^{-1}$ ]
$\lambda$	Bulk viscosity [ $\text{kg}\cdot\text{m}^{-1}\cdot\text{s}^{-1}$ ]
$\tau$	Shear stress [ $\text{N}\cdot\text{m}^{-2}$ ]
g	Gravitational acceleration [ $\text{m}\cdot\text{s}^{-2}$ ]
$e_s$	Restitution coefficient []
$g_0$	Radial distribution function []
$\theta$	Granular temperature [ $\text{m}^2\cdot\text{s}^{-2}$ ]
k	Turbulent kinetic energy [ $\text{m}^2\cdot\text{s}^{-2}$ ]
$\gamma$	Dissipation of granular energy [ $\text{kg}\cdot\text{s}^{-3}\cdot\text{m}^{-1}$ ]
$\phi$	Energy exchange [ $\text{kg}\cdot\text{s}^{-3}\cdot\text{m}^{-1}$ ]
d	Diameter [m]
$C_p$	Heat capacity [ $\text{kg}\cdot\text{m}^2\cdot\text{k}^{-1}\cdot\text{s}^{-2}$ ]
$C_D$	Drag coefficient []
T	Temperature [k]
$m_p$	Mass flow rate [ $\text{kg}\cdot\text{s}^{-1}$ ]
h	Heat transfer coefficient [ $\text{w}\cdot\text{m}^{-2}\cdot\text{k}^{-1}$ ]
A	Surface area [ $\text{m}^2$ ]
$\bar{I}$	Unit tensor []
<b>Subscript</b>	
s	Solid
l	Liquid
g	gas

1

2

3

1  
2  
3  
4  
5  
6  
7  
8  
9  
10  
11  
12  
13  
14  
15  
16  
17  
18  
19  
20  
21  
22  
23

#### References

Antony, J., Shyamkumar, M., 2016. Study on Sand Particles Drying in a Fluidized Bed Dryer using CFD. *International Journal of Engineering* 8, 129-145.

Arastoopour, H., Gidaspow, D., Abbasi, E., 2017. *Computational Transport Phenomena of Fluid-Particle Systems*. Springer.

Aust, R., Durst, F., Raszillier, H., 1997. Modeling a multiple-zone air impingement dryer. *Chemical Engineering and Processing: Process Intensification* 36, 469-487.

Baker, C., 1988. The design of flights in cascading rotary dryers. *Drying Technology* 6, 631-653.

Baker, C., McKenzie, K., 2005. Energy consumption of industrial spray dryers. *Drying Technology* 23, 365-386.

Devahastin, S., Mujumdar, A.S., 2007. Indirect dryers. *Handbook of Industrial Drying*, 127-137.

Fries, L., Antonyuk, S., Heinrich, S., Palzer, S., 2011. DEM–CFD modeling of a fluidized bed spray granulator. *Chemical Engineering Science* 66, 2340-2355.

Ghadirian, E., Abbasian, J., Arastoopour, H., 2019. CFD simulation of gas and particle flow and a carbon capture process using a circulating fluidized bed (CFB) reacting loop. *Powder technology* 344, 27-35.

Gidaspow, D., Bezburuah, R., Ding, J., 1991. *Hydrodynamics of circulating fluidized beds: kinetic theory approach*. Illinois Inst. of Tech., Chicago, IL (United States). Dept. of Chemical Engineering.

Gunn, D., 1978. Transfer of heat or mass to particles in fixed and fluidised beds. *International Journal of Heat and Mass Transfer* 21, 467-476.

- 1 Hepbasli, A., Colak, N., Hancioglu, E., Icier, F., Erbay, Z., 2010. Exergoeconomic analysis of plum drying  
2 in a heat pump conveyor dryer. *Drying Technology* 28, 1385-1395.
- 3 Hovmand, S., 1995. Fluidized bed drying. *Handbook of industrial drying* 1, 195-248.
- 4 Huang, A.-N., Kuo, H.-P., 2018. CFD simulation of particle segregation in a rotating drum. Part II: Effects  
5 of specular coefficient. *Advanced Powder Technology* 29, 3368-3374.
- 6 Jamaledine, T.J., Ray, M.B., 2010. Application of computational fluid dynamics for simulation of drying  
7 processes: A review. *Drying Technology* 28, 120-154.
- 8 Khomwachirakul, P., Devahastin, S., Swasdisevi, T., Soponronnarit, S., 2016. Simulation of flow and  
9 drying characteristics of high-moisture particles in an impinging stream dryer via CFD-DEM. *Drying*  
10 *Technology* 34, 403-419.
- 11 Korn, O., 2001. Cyclone dryer: A pneumatic dryer with increased solid residence time. *Drying Technology*  
12 19, 1925-1937.
- 13 Manickavasagan, A., Jayas, D., White, N., 2006. Non-uniformity of surface temperatures of grain after  
14 microwave treatment in an industrial microwave dryer. *Drying Technology* 24, 1559-1567.
- 15 Mujumdar, A.S., 1995. Superheated steam drying. *Handbook of industrial drying* 2, 1071-1086.
- 16 Mujumdar, A.S., 2006. *Handbook of industrial drying*. CRC press.
- 17 Ng, B., Ding, Y., Ghadiri, M., 2009. Modelling of dense and complex granular flow in high shear mixer  
18 granulator—a CFD approach. *Chemical engineering science* 64, 3622-3632.
- 19 Ochieng, A., Onyango, M.S., 2008. Drag models, solids concentration and velocity distribution in a stirred  
20 tank. *Powder Technology* 181, 1-8.
- 21 Pangavhane, D.R., Sawhney, R., Sarsavadia, P., 2002. Design, development and performance testing of a  
22 new natural convection solar dryer. *Energy* 27, 579-590.
- 23 Pasquini, N., Addeo, A., 2005. *Polypropylene handbook*.

- 1 Pubns, H.G., 1996. Polypropylene handbook: polymerization, characterization, properties, processing,  
2 applications.
- 3 Rafique, M., Chen, P., Duduković, M., 2004. Computational modeling of gas-liquid flow in bubble  
4 columns. *Reviews in Chemical Engineering* 20, 225-375.
- 5 Sadin, R., Chegini, G.-R., Sadin, H., 2014. The effect of temperature and slice thickness on drying kinetics  
6 tomato in the infrared dryer. *Heat and Mass Transfer* 50, 501-507.
- 7 Schiffmann, R.F., 1995. Microwave and dielectric drying. *Handbook of industrial drying* 1, 345-372.
- 8 Schiller, L., Naumann, A., A drag coefficient correlation. *Vdi Zeitung*, 77: 318–320, 1935. Cité page 38.
- 9 Sokolichin, A., Eigenberger, G., Lapin, A., 2004. Simulation of buoyancy driven bubbly flow: established  
10 simplifications and open questions. *AIChE Journal* 50, 24-45.
- 11 Szafran, R.G., Kmiec, A., 2004. CFD Modeling of Heat and Mass Transfer in a Spouted Bed Dryer.  
12 *Industrial & Engineering Chemistry Research* 43, 1113-1124.
- 13 Szafran, R.G., Kmiec, A., Ludwig, W., 2005. CFD Modeling of a Spouted-Bed Dryer Hydrodynamics.  
14 *Drying Technology* 23, 1723-1736.
- 15 Tang, J., Feng, H., Shen, G.-Q., 2003. Drum drying, *Encyclopaedia of Agricultural, Food, and Biological*  
16 *Engineering*. Marcel Dekker, Inc., New York, pp. 211-214.
- 17 Tang, X.C., Nail, S.L., Pikal, M.J., 2005. Freeze-drying process design by manometric temperature  
18 measurement: design of a smart freeze-dryer. *Pharmaceutical research* 22, 685-700.
- 19 Wang, H., Yang, W., Senior, P., Raghavan, R., Duncan, S., 2008. Investigation of batch fluidized-bed  
20 drying by mathematical modeling, CFD simulation and ECT measurement. *AIChE Journal* 54, 427-444.
- 21 Zhonghua, W., Mujumdar, A.S., 2008. CFD modeling of the gas–particle flow behavior in spouted beds.  
22 *Powder Technology* 183, 260-272.

23